

# Quantum information spreading in generalised dual-unitary circuits

Alessandro Foligno,<sup>1,2</sup> Pavel Kos,<sup>3</sup> and Bruno Bertini<sup>1,2</sup>

<sup>1</sup>*School of Physics and Astronomy, University of Nottingham, Nottingham, NG7 2RD, UK*

<sup>2</sup>*Centre for the Mathematics and Theoretical Physics of Quantum*

*Non-Equilibrium Systems, University of Nottingham, Nottingham, NG7 2RD, UK*

<sup>3</sup>*Max-Planck-Institut für Quantenoptik, Hans-Kopfermann-Str. 1, 85748 Garching*

We study the spreading of quantum information in a recently introduced family of brickwork quantum circuits that generalises the dual-unitary class. These circuits are unitary in time, while their spatial dynamics is unitary only in a restricted subspace. First, we show that local operators spread at the speed of light as in dual-unitary circuits, i.e., the butterfly velocity takes the maximal value allowed by the geometry of the circuit. Then, we prove that the entanglement spreading can still be characterised exactly for a family of compatible initial states (in fact, for an extension of the compatible family of dual-unitary circuits) and that the asymptotic entanglement slope is again independent on the Rényi index. Remarkably, however, we find that the entanglement velocity is generically smaller than one. We use these properties to find a closed-form expression for the entanglement membrane in these circuits.

In recent years, quantum circuits have emerged as useful effective models to understand generic, or “chaotic”, quantum many-body dynamics [1–13]. The most appealing feature of these systems is that, contrary to generic many-body systems in continuous time, their dynamics are sometimes amenable to analytical descriptions. The latter feature is particularly significant in light of the current lack of computational approaches able to efficiently characterise out-of-equilibrium quantum matter.

The approaches followed to obtain analytical insights in quantum circuits can be divided in two groups. The first involves introducing a certain degree of randomness in the system to simplify the theoretical description [2, 5, 14]. This approach is inspired by random matrix theory [15] and has its most representative example in Haar-random circuits [2], which have been used to obtain several important results on operator dynamics, information spreading, and spectral statistics [2–6, 9–11, 14, 16–25]. The second route, instead, is to derive exact results for special classes of systems obtained by imposing certain conditions on the elementary quantum gates without affecting the nature of the dynamics [8, 26–31]. The appeal of this second approach is that it is arguably more fundamental — it allows one to study truly closed quantum many-body systems — and its most representative example is that of dual-unitary (DU) circuits [8].

The defining property of the latter systems is that their local gates remain unitary upon exchanging the roles of space and time. This allows for the analytic treatment of quantities notoriously hard to compute in general (examples include out-of-time correlators (OTOCs) [32–35], entanglement growth after quantum quenches [7, 36–38], spectral form factor [3, 39], temporal entanglement [40, 41], operator entanglement [34, 42–44], deep thermalization [45–47], and tripartite information [33]), however, it does not modify the chaotic nature of the dynamics. The only macroscopic effect of dual unitarity is that it enforces maximal velocity for the spreading of quantum correlations. Specifically, in DU circuits both

the butterfly velocity characterising operator spreading and the entanglement velocity of any state are equal to the speed of light [32, 37, 38]. In fact, the second property alone implies conversely the dual unitarity [48].

The fact that both scrambling and thermalisation occur at the fastest possible rate in DU circuits leaves a distinct mark on the dynamics of quantum information. This is true even at the coarse grained level where quantum information spreading in chaotic systems is described by the so called entanglement membrane [18, 24, 25] (see also [49, 50]), which in DU circuits has been shown to exhibit an extremal, constant line tension [18]. The natural question is then whether the dual unitarity condition can somehow be weakened, leading to a more generic, yet solvable, quantum information flow.

In this Letter we address this question by characterising the dynamics of quantum information in a class of “hierarchical generalisations” of DU circuits recently proposed in Ref. [51]. The idea is to construct a hierarchy of multi-gate conditions, where going up in the hierarchy corresponds to weakening more and more the constraint imposed on a single gate, with dual unitarity being at the bottom as the strongest one. Here we consider the second hierarchy of generalisations, DU2 from now on, and find the following results. First, the butterfly velocity continues to be equal to one (in fact we show that this is true for all levels of the hierarchy of Ref. [51]). Second, the entanglement velocity is still independent on the Rényi index and can still be computed exactly. It is, however, generically *sub-maximal* and takes discrete values depending on the local Hilbert space dimension. Finally, we recover these results by computing the entanglement membrane of DU2 and finding that it has non-trivial line tension. To the best of our knowledge the one provided here is the first explicit expression for a non-constant line tension derived in a clean, interacting microscopic system.

More specifically, we consider a one-dimensional quantum circuit, made of  $2L$  sites of qudits (quantum systems with  $d$  internal states), with a discrete, local unitary evo-

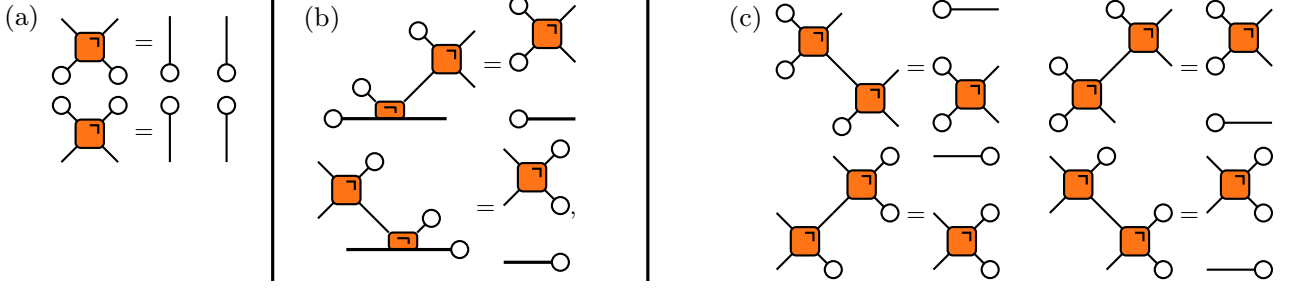


FIG. 1: Graphical representations of unitarity (left), compatibility relations for the initial state (cf. Eq. 15) (center), and DU2 conditions (cf. Eq. (2)), (top right). The relations on the bottom of (c) are equivalent to those on the top [51].

lution. Neighbouring sites are by definition at distance of  $1/2$  apart, and their positions, labelled by half-integers, take periodic values on a ring of length  $L$  (the qudit at position 0 is the same as the one at position  $L$ ). A single time step is determined by the following unitary operator  $\mathbb{U} = \mathbb{U}_e \mathbb{U}_o$  with

$$\mathbb{U}_e = \bigotimes_{x \in \mathbb{Z}_L} U_{x, x+1/2}, \quad \mathbb{U}_o = \bigotimes_{x \in \mathbb{Z}_L} U_{x-1/2, x}, \quad (1)$$

$U_{a,b}$  is a two site unitary gate which acts on sites  $a, b$ .

We consider a subclass of unitary gates fulfilling the DU2 conditions [51]. These can be expressed by defining a spacetime swapped gate  $\tilde{U}$  as  $\langle kl | \tilde{U} | ij \rangle = \langle lj | U | ki \rangle$ . In terms of these gates the DU2 condition becomes (see also Fig. 1)

$$\begin{aligned} (\tilde{U} \otimes \mathbb{1}_d) (\mathbb{1}_d \otimes \tilde{U} \tilde{U}^\dagger) (\tilde{U}^\dagger \otimes \mathbb{1}_d) &= \tilde{U} \tilde{U}^\dagger \otimes \mathbb{1}_d, \\ (\mathbb{1}_d \otimes \tilde{U}) (\tilde{U} \tilde{U}^\dagger \otimes \mathbb{1}_d) (\mathbb{1}_d \otimes \tilde{U}^\dagger) &= \mathbb{1}_d \otimes \tilde{U} \tilde{U}^\dagger, \end{aligned} \quad (2)$$

where  $\mathbb{1}_x$  is the identity on a space of dimension  $x$ . This property is satisfied for DU gates where  $\tilde{U}$  is unitary, however, it admits also families of non-DU solutions [51]. Note that Eq. (2) implies the validity of the equivalent set of relations with  $\tilde{U}^\dagger$  and  $\tilde{U}$  exchanged [51].

Let us begin considering the speed of operator spreading, i.e. the *butterfly velocity*  $v_B$ , in DU2 circuits. The latter can be quantified by looking at the following OTOC

$$O_{\alpha\beta}(x, t) = 1 - \frac{1}{d^{2L}} \text{tr} \left[ \sigma_0^{(\alpha)}(t) \sigma_x^{(\beta)}(0) \sigma_0^{(\alpha)}(t) \sigma_x^{(\beta)}(0) \right], \quad (3)$$

where  $\{\sigma^{(\alpha)}\}_{\alpha=1, \dots, d^2-1}$  are a basis for local traceless hermitian operators [52]. In chaotic systems, this OTOC approaches asymptotically one for  $|x| \leq v_B t$ , and 0 otherwise. In particular, Haar random circuits have  $v_B = (d^2 - 1)/(d^2 + 1)$  [4, 6], while DU circuits  $v_B = 1$  [32, 33]. Note that the latter is the largest possible  $v_B$  because the strict causality encoded in Eq. (1) assures  $O_{\alpha\beta}(x, t) = 0$  for  $|x| > t$ .

To compute  $v_B$  for DU2 we use the strategy of Refs. [32, 33]. Namely, we compute the limit  $x, t \rightarrow \infty$

with  $x_- = t - x$  fixed: if  $O_{\alpha\beta}(x, t)$  is non-zero in this limit we have  $v_B = 1$  otherwise  $v_B < 1$  [53]. The limit is conveniently computed writing  $1 - O_{\alpha\beta}(x, t)$  in terms of a suitable transfer matrix and expressing its asymptotic scaling in terms of the transfer-matrix fixed points. This procedure becomes particularly transparent by introducing a diagrammatic representation, similar to the one used in tensor networks, where one depicts single local gates as boxes with legs corresponding to the qudits they act on, see e.g. [8, 33, 36]. In particular, since here we are interested in multi replica quantities we consider a graphical representation of “folded” quantum gates, i.e., tensor products of 2 replicas of  $U$  and its hermitian conjugate

$$\text{Square gate with four legs} \equiv (U \otimes U^*)^{\otimes 2}. \quad (4)$$

The Hilbert spaces associated to each leg have dimension  $d^4$ . For  $|x| < t$  one can express the quantity of interest in terms of (4) as follows [54]

$$1 - O_{\alpha\beta}(x, t) = \frac{1}{d^{2t}} \text{tr} \left[ \text{Diagrammatic representation of } 1 - O_{\alpha\beta}(x, t) \right]. \quad (5)$$

Here  $x_{\pm} = t \pm x$ , joined legs imply matrix product and we introduced a graphical representation for two different index contractions that can be seen as states in the replicated Hilbert space, i.e.

$$|\bigcirc\rangle = \sum_{i,j=1}^d |ijj\rangle, \quad |\square\rangle = \sum_{i,j=1}^d |ijji\rangle, \quad (6)$$

where we used the shorthand notation  $|i_1 i_2 i_3 i_4\rangle \equiv |i_1\rangle \otimes |i_2\rangle \otimes |i_3\rangle \otimes |i_4\rangle$ . Note that these states are neither orthogonal nor normalised and one has  $\langle \bigcirc | \square \rangle = d$  and



The physical meaning of (17) is that for early times ( $4t \leq L_A + 2t \leq L$ ) the entanglement between  $A$  and the rest is only produced at the two edges between the two subsystems and the latter are independent as expected by causality [56].

Next we observe that, by repeated applications of the DU2 property (cf. Fig. 1) and the diagrammatic version of the compatibility condition (15) (Fig. 1b and c) we have

$$= \text{[Diagram of a single orange square with four white circles]} \quad (20)$$

This gives the following asymptotic entanglement velocity

$$\begin{aligned} v_E^{(n)} &\equiv \lim_{t \rightarrow \infty} \lim_{L_A \rightarrow \infty} \lim_{L \rightarrow \infty} \frac{S_A^{(n)}(t)}{4t \log(d)} = \\ &= 1 + \frac{\log(\text{tr}[(\tilde{U}\tilde{U}^\dagger)^n]/d^2)}{2(1-n)\log(d)}. \end{aligned} \quad (21)$$

This result generalises the one found for DU circuits [7, 37], i.e.  $v_E^{(n)} = 1$ , which is recovered setting  $\tilde{U}\tilde{U}^\dagger = \mathbb{1}_{d^2}$ . Remarkably, however, Eq. (21) continues to be  $n$  independent for all DU2 circuits. Indeed, as we show in the SM, the spectrum of the matrix  $\tilde{U}\tilde{U}^\dagger$  is constant for all DU2 gates. Namely, we have the following property [55]

**Property 1.** *For DU2 circuits the eigenvalues of  $\tilde{U}\tilde{U}^\dagger$  are all either equal to 0 or to a positive constant  $\Lambda^2$ .*

Since the trace of  $\tilde{U}\tilde{U}^\dagger$  is fixed by the unitarity of  $U$ , the dimension of the non-trivial eigenspace,  $n_\Lambda = 1, \dots, d^2$ , is such that  $n_\Lambda \Lambda^2 = d^2$ . This allows us to rewrite Eq. (21) as

$$v_E^{(n)} = \frac{\log(\frac{d}{\Lambda})}{\log(d)} = \frac{\log(n_\Lambda)}{2\log(d)}, \quad n_\Lambda = 1, \dots, d^2. \quad (22)$$

This exact expression for the entanglement velocity represents our second main result.

We now recover our exact results using the entanglement membrane picture [18, 24, 25]. The idea of this approach is that the entanglement can be viewed as the energy of a coarse-grained curve (that only depends on its slope). This means that one can write a Rényi entropy as [24]

$$S_n(x, t) = \min_y \left( \mathcal{E}_n \left( \frac{x-y}{t} \right) + S_n(y, 0) \right). \quad (23)$$

The function  $\mathcal{E}_n(v)$  can be computed by evaluating the scaling limit of a suitable matrix element in the replicated

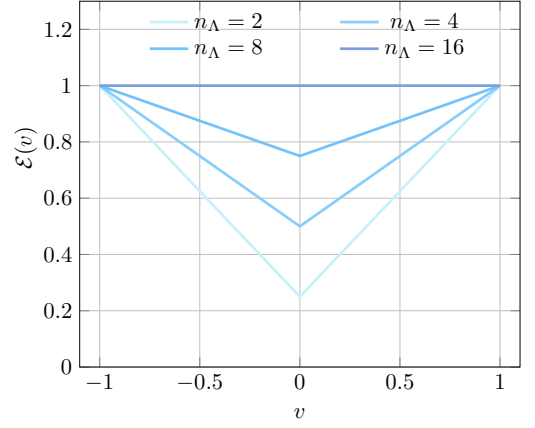


FIG. 2: Entanglement membrane line tension of DU2 circuits [cf. Eq. (26)], for  $d = 4$ , and  $n_\Lambda$  taking all possible values (except the trivial value 1) corresponding to different choices of DU2 gates.

space [18]. Namely we have

$$\begin{aligned} &\lim_{L \rightarrow \infty} \frac{\langle \overbrace{\square \cdots \square}^{L-2vt} \cdots \square \circ \cdots \circ (U(t) \otimes U(t)^*)^{\otimes n} \overbrace{\square \cdots \square}^L \cdots \square \circ \cdots \circ \rangle}{d^{2nL}} \\ &\simeq \exp((1-n)t\mathcal{E}_n(v)\log d), \end{aligned} \quad (24)$$

where  $\simeq$  denotes equality at leading order in  $t$ . The matrix element on the l.h.s. is typically very hard to evaluate analytically and closed form expressions have only been found in the presence of randomness and for large  $d$  [24, 25, 57], in the dual-unitary case [18], or for holographic quantum field theories [58]. In this case, instead, the calculation is straightforward. Graphically, Eq. (24) corresponds to

$$e^{\frac{t\mathcal{E}_n(v)\log d}{(1-n)^{-1}}} \simeq \frac{1}{d^{2nt}} \text{[Diagram]}, \quad (25)$$

and can be explicitly contracted using the DU2 property (cf. Fig. 1) starting from the top-left and bottom-right corners. This leads to the following closed-form expression

$$\mathcal{E}_n(v) = \left( |v| + \frac{1-|v|}{2} \frac{\log(n_\Lambda)}{\log(d)} \right). \quad (26)$$

We see that  $\mathcal{E}_n(v)$  shows a non-trivial dependence on  $v$  but is convex as it should be for consistency. Specifically, it is generically linear in  $|v|$  and becomes constant only in the DU case  $n_\Lambda = d^2$  (see Fig. 2). As shown in Ref. [58], this form maximises the entanglement growth for fixed

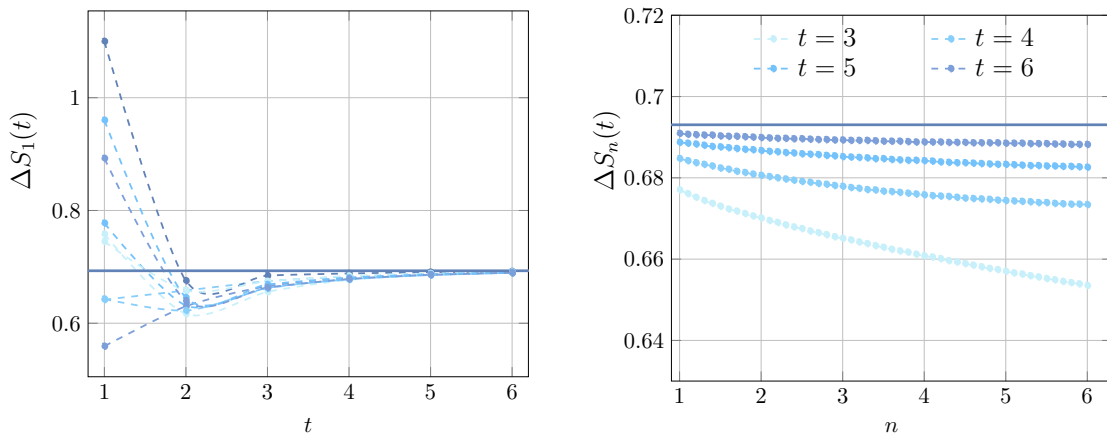


FIG. 3: Left: Entanglement slopes from random dimer-product states (products of entangled states of two qudits), compared with the expected slope from solvable states (solid line). Right: Slope of Rényi entropies for various values of  $t$  as a function of the Rényi index  $n$ , compared to the  $n$ -independent result from solvable states (solid line).

$v_E$  and  $v_B$ . Eq. (26) allows us one to recover our exact results for butterfly and entanglement velocity within the membrane approach [24]: the solution to  $\mathcal{E}(v) = v$  is indeed  $v = v_B = 1$  and  $v_E^{(n)} = \mathcal{E}(v = 0)$  coincides with Eq. (22). In fact, the membrane approach suggests that this result does not depend on the initial state chosen, as long as it is low entangled, and should apply also for states that do not satisfy the conditions (15). In Fig. 3 we test numerically this prediction finding convincing agreement.

In this Letter we presented an explicit characterisation of the quantum information flow in a class of unitary circuits, dubbed DU2 circuits, that generalises that of dual unitary circuits. We showed that, although local operators in the vacuum spread at the maximal speed and the entanglement spectrum after a quench is asymptotically flat, the entanglement velocity is submaximal and its value depends on additional properties of the gate. Finally, by deriving an exact expression for the line tension, we showed that these results can be recovered using the entanglement membrane approach.

Our exact results put DU2 circuits forward as a more general class of solvable, yet chaotic, quantum circuits

and pave the way for many directions of future research. Some natural questions are whether one can construct instances of chaotic DU2 circuits with non-trivial conservation laws or devise exactly solvable measurement protocols in these circuits. Another interesting question is whether there exist subclasses of DU2 circuits generating low temporal entanglement after quenches from generic initial states.

*Note Added.* While this manuscript was being finalised, we became aware of the related work [59], which will soon appear on arXiv.

#### ACKNOWLEDGMENTS

We thank Katja Klobas for collaboration in the early stages of this project and for valuable comments on the manuscript. We also thank Xie-Hang Yu for useful discussions. We acknowledge financial support from the Royal Society through the University Research Fellowship No. 201101 (A. F. and B. B.). P. K. is supported by the Alexander von Humboldt Foundation. We warmly acknowledge the hospitality of the Simons Center for Geometry and Physics during the program “Fluctuations, Entanglements, and Chaos: Exact Results” where part of this work has been performed.

- 
- [1] P. Hosur, X.-L. Qi, D. A. Roberts, and B. Yoshida, Chaos in quantum channels, *Journal of High Energy Physics* **2016**, 1 (2016).
  - [2] A. Nahum, J. Ruhman, S. Vijay, and J. Haah, Quantum entanglement growth under random unitary dynamics, *Phys. Rev. X* **7**, 031016 (2017).
  - [3] B. Bertini, P. Kos, and T. Prosen, Exact spectral form factor in a minimal model of many-body quantum chaos, *Phys. Rev. Lett.* **121**, 264101 (2018).
  - [4] A. Nahum, S. Vijay, and J. Haah, Operator spreading in random unitary circuits, *Phys. Rev. X* **8**, 021014 (2018).
  - [5] A. Chan, A. De Luca, and J. T. Chalker, Solution of a minimal model for many-body quantum chaos, *Phys. Rev. X* **8**, 041019 (2018).
  - [6] C. W. von Keyserlingk, T. Rakovszky, F. Pollmann, and S. L. Sondhi, Operator Hydrodynamics, OTOCs, and Entanglement Growth in Systems without Conservation Laws, *Phys. Rev. X* **8**, 021013 (2018).
  - [7] B. Bertini, P. Kos, and T. Prosen, Entanglement spreading in a minimal model of maximal many-body quantum chaos, *Phys. Rev. X* **9**, 021033 (2019).
  - [8] B. Bertini, P. Kos, and T. Prosen, Exact correlation func-

- tions for dual-unitary lattice models in  $1+1$  dimensions, *Phys. Rev. Lett.* **123**, 210601 (2019).
- [9] A. J. Friedman, A. Chan, A. De Luca, and J. T. Chalker, Spectral statistics and many-body quantum chaos with conserved charge, *Phys. Rev. Lett.* **123**, 210603 (2019).
- [10] Y. Li, X. Chen, and M. P. A. Fisher, Measurement-driven entanglement transition in hybrid quantum circuits, *Phys. Rev. B* **100**, 134306 (2019).
- [11] B. Skinner, J. Ruhman, and A. Nahum, Measurement-induced phase transitions in the dynamics of entanglement, *Phys. Rev. X* **9**, 031009 (2019).
- [12] T. Rakovszky, F. Pollmann, and C. W. von Keyserlingk, Sub-ballistic growth of Rényi entropies due to diffusion, *Phys. Rev. Lett.* **122**, 250602 (2019).
- [13] A. Zabalo, M. J. Gullans, J. H. Wilson, S. Gopalakrishnan, D. A. Huse, and J. H. Pixley, Critical properties of the measurement-induced transition in random quantum circuits, *Phys. Rev. B* **101**, 060301(R) (2020).
- [14] M. P. A. Fisher, V. Khemani, A. Nahum, and S. Vijay, Random quantum circuits, *arXiv:2207.14280* (2022).
- [15] M. Mehta, *Random Matrices* (Academic Press, 1991).
- [16] V. Khemani, A. Vishwanath, and D. A. Huse, Operator spreading and the emergence of dissipative hydrodynamics under unitary evolution with conservation laws, *Phys. Rev. X* **8**, 031057 (2018).
- [17] T. Rakovszky, F. Pollmann, and C. W. von Keyserlingk, Diffusive hydrodynamics of out-of-time-ordered correlators with charge conservation, *Phys. Rev. X* **8**, 031058 (2018).
- [18] T. Zhou and A. Nahum, Entanglement membrane in chaotic many-body systems, *Phys. Rev. X* **10**, 031066 (2020).
- [19] H. Wang and T. Zhou, Barrier from chaos: operator entanglement dynamics of the reduced density matrix, *JHEP* **2019** (12), 1.
- [20] A. Chan, R. M. Nandkishore, M. Pretko, and G. Smith, Unitary-projective entanglement dynamics, *Phys. Rev. B* **99**, 224307 (2019).
- [21] A. Chan, A. De Luca, and J. T. Chalker, Spectral statistics in spatially extended chaotic quantum many-body systems, *Phys. Rev. Lett.* **121**, 060601 (2018).
- [22] S. J. Garratt and J. T. Chalker, Many-body delocalization as symmetry breaking, *Phys. Rev. Lett.* **127**, 026802 (2021).
- [23] S. J. Garratt and J. T. Chalker, Local pairing of Feynman histories in many-body Floquet models, *Phys. Rev. X* **11**, 021051 (2021).
- [24] C. Jonay, D. A. Huse, and A. Nahum, Coarse-grained dynamics of operator and state entanglement, *arXiv:1803.00089* (2018).
- [25] T. Zhou and A. Nahum, Emergent statistical mechanics of entanglement in random unitary circuits, *Phys. Rev. B* **99**, 174205 (2019).
- [26] K. Klobas, B. Bertini, and L. Piroli, Exact thermalization dynamics in the “Rule 54” quantum cellular automaton, *Phys. Rev. Lett.* **126**, 160602 (2021).
- [27] T. Prosen, Many-body quantum chaos and dual-unitarity round-a-face, *Chaos: An Interdisciplinary Journal of Nonlinear Science* **31**, 033101 (2021), <https://doi.org/10.1063/5.0056970>.
- [28] P. Kos, B. Bertini, and T. Prosen, Correlations in perturbed dual-unitary circuits: Efficient path-integral formula, *Phys. Rev. X* **11**, 011022 (2021).
- [29] B. Bertini, P. Kos, and T. Prosen, Exact spectral statistics in strongly localized circuits, *Phys. Rev. B* **105**, 165142 (2022).
- [30] P. Kos and G. Styliaris, Circuits of space and time quantum channels, *Quantum* **7**, 1020 (2023).
- [31] B. Bertini, C. De Fazio, J. P. Garrahan, and K. Klobas, Exact quench dynamics of the Floquet quantum East model at the deterministic point, *arXiv:2310.06128* (2023).
- [32] P. W. Claeys and A. Lamacraft, Maximum velocity quantum circuits, *Phys. Rev. Research* **2**, 033032 (2020).
- [33] B. Bertini and L. Piroli, Scrambling in random unitary circuits: Exact results, *Phys. Rev. B* **102**, 064305 (2020).
- [34] N. Dowling, P. Kos, and K. Modi, Scrambling is necessary but not sufficient for chaos, *Phys. Rev. Lett.* **131**, 180403 (2023).
- [35] M. A. Rampp, R. Moessner, and P. W. Claeys, From dual unitarity to generic quantum operator spreading, *Phys. Rev. Lett.* **130**, 130402 (2023).
- [36] S. Gopalakrishnan and A. Lamacraft, Unitary circuits of finite depth and infinite width from quantum channels, *Phys. Rev. B* **100**, 064309 (2019).
- [37] L. Piroli, B. Bertini, J. I. Cirac, and T. Prosen, Exact dynamics in dual-unitary quantum circuits, *Phys. Rev. B* **101**, 094304 (2020).
- [38] A. Foligno and B. Bertini, Growth of entanglement of generic states under dual-unitary dynamics, *Phys. Rev. B* **107**, 174311 (2023).
- [39] B. Bertini, P. Kos, and T. Prosen, Random matrix spectral form factor of dual-unitary quantum circuits, *Commun. Math. Phys.*, 1 (2021).
- [40] G. Giudice, G. Giudici, M. Sonner, J. Thoenness, A. Lerose, D. A. Abanin, and L. Piroli, Temporal entanglement, quasiparticles, and the role of interactions, *Phys. Rev. Lett.* **128**, 220401 (2022).
- [41] A. Foligno, T. Zhou, and B. Bertini, Temporal entanglement in chaotic quantum circuits, *Phys. Rev. X* **13**, 041008 (2023).
- [42] B. Bertini, P. Kos, and T. Prosen, Operator Entanglement in Local Quantum Circuits I: Chaotic Dual-Unitary Circuits, *SciPost Phys.* **8**, 67 (2020).
- [43] B. Bertini, P. Kos, and T. Prosen, Operator entanglement in local quantum circuits ii: Solitons in chains of qubits, *SciPost Physics* **8**, 68 (2020).
- [44] I. Reid and B. Bertini, Entanglement barriers in dual-unitary circuits, *Phys. Rev. B* **104**, 014301 (2021).
- [45] W. W. Ho and S. Choi, Exact emergent quantum state designs from quantum chaotic dynamics, *Phys. Rev. Lett.* **128**, 060601 (2022).
- [46] P. W. Claeys and A. Lamacraft, Emergent quantum state designs and biunitarity in dual-unitary circuit dynamics, *Quantum* **6**, 738 (2022).
- [47] M. Ippoliti and W. W. Ho, Solvable model of deep thermalization with distinct design times, *Quantum* **6**, 886 (2022).
- [48] T. Zhou and A. W. Harrow, Maximal entanglement velocity implies dual unitarity, *Phys. Rev. B* **106**, L201104 (2022).
- [49] T. Zhou and J. Virrueta, Exploring the membrane theory of entanglement dynamics, *Journal of High Energy Physics* **2020**, 1 (2020).
- [50] C. A. Agón and M. Mezei, Bit threads and the membrane theory of entanglement dynamics, *Journal of High Energy Physics* **2021**, 1 (2021).

- [51] X.-H. Yu, Z. Wang, and P. Kos, Hierarchical generalization of dual unitarity, arXiv:2307.03138 (2023).
- [52] We take them to be orthogonal with respect to the Hilbert-Schmidt product, i.e.,  $\text{tr}[\sigma^{(\alpha)}\sigma^{(\beta)}] = d\delta_{\alpha,\beta}$ .
- [53] Here we assume parity symmetry. If there is no parity symmetry one has to consider also the limit  $|x|, t \rightarrow \infty$  with  $x_+ = t + x$  fixed. The treatment is completely analogous.
- [54] In Eq. (5) we assumed  $x$  to be half-integer; the case of integer  $x$  leads to identical considerations.
- [55] See the Supplemental Material for: (i) an explicit calculation of the scalar product in Eq. (12); (ii) A characterisation of Rényi entropies at early times, i.e., for  $L \geq L_A + 2t \geq 4t$  and a proof of Eq. (17); (iii) A proof that the matrix  $\tilde{U}\tilde{U}^\dagger$  has flat spectrum; (iv) The parameterisation considered in our numerical experiments.
- [56] B. Bertini, K. Klobas, and T.-C. Lu, Entanglement negativity and mutual information after a quantum quench: Exact link from space-time duality, Phys. Rev. Lett. **129**, 140503 (2022).
- [57] Z. Gong, A. Nahum, and L. Piroli, Coarse-grained entanglement and operator growth in anomalous dynamics, Phys. Rev. Lett. **128**, 080602 (2022).
- [58] M. Mezei, Membrane theory of entanglement dynamics from holography, Phys. Rev. D **98**, 106025 (2018).
- [59] M. Rampp, S. Rather, and P. W. Claeys, arXiv:2312.XXXXX (2023).

## Supplemental Material: Information spreading in generalised dual-unitary circuits

Here we report some useful information complementing the main text. In particular

- In Sec. I we compute explicitly the scalar products  $\langle l|\blacksquare\rangle = \langle \bullet|r\rangle$  in Eq. (12) of the main text.
- In Sec. II we characterise Rényi entropies at early times, i.e., for  $L \geq L_A + 2t \geq 4t$  and prove Eq. (17) of the main text.
- In Sec. III we show that the matrix  $\tilde{U}\tilde{U}^\dagger$  has flat spectrum.
- In Sec. IV we report the parameterisation used for our numerical experiments.

### I. EXPLICIT CALCULATION OF THE SCALAR PRODUCT IN EQ. (12)

Consider the vectors  $|l\rangle$  and  $|\blacksquare\rangle$  in Eqs. (10) and (11). Their scalar product can be compute by decomposing  $|\blacksquare\rangle$

$$\langle l|\blacksquare\rangle = d\langle l|\bigcirc\rangle - \langle l|\square\rangle = d \text{ (diagram 1) } - \text{ (diagram 2) }. \quad (27)$$

The first term can be immediately simplified using unitarity and obtaining  $d^4$ , while the second one can be written in terms of  $\tilde{U}$  as

$$\langle l|\bullet\rangle = d^4 - \text{tr} \left[ \left( \tilde{U}\tilde{U}^\dagger \right)^2 \right] = d^4 \left( 1 - \frac{1}{n_A} \right), \quad (28)$$

where we used Eq. (50) to simplify the second term; identical considerations apply to  $\langle \blacksquare|r\rangle$ .

### II. ENTANGLEMENT DYNAMICS AT EARLY TIMES

In order to compute the Rényi entropy from Eq. (16), we can express the trace of the  $n$ -th power of the reduced density matrix as a contracted network, if we consider a  $2n$  folded gate

$$(U \otimes U^*)^{\otimes n} = \text{ (diagram of a folded gate) } \quad (29)$$

$$\begin{aligned} \text{tr} [\rho_A^n] &= \frac{1}{d^{nL}} \text{ (diagram of a long chain of folded gates) } \\ &= \frac{1}{d^{nL}} \dots \underbrace{\text{ (diagram of a folded gate) }}_{2t+1} \underbrace{\text{ (diagram of a folded gate) }}_{2t+1} \dots, \end{aligned} \quad (30)$$

where now the states  $|\bigcirc\rangle, |\square\rangle$  represent two different contractions in the space of replicas, defined as in (18). Equation (30) can be further simplified, by noting that the matrix MPS transfer matrix has an eigenvalue fixed by the compatibility condition (15). Using the unitarity of the gate, it is easy to show that

$$\text{ (diagram 1) } = d^n \text{ (diagram 2) } \quad \text{ (diagram 3) } = d^n \text{ (diagram 4) }, \quad (31)$$

where, due to the global replica symmetry, the same relation holds if we replace all the circles with squares. If we assume this eigenvalue of the transfer matrix is unique and maximal, then we can further simplify (30) as

$$\text{tr} [\rho_A^n] = \frac{1}{\chi^n d^{n(L_A+2t+1)}} \underbrace{\text{Diagram 1}}_{2t+1} \underbrace{\text{Diagram 2}}_{2t+1}. \quad (32)$$

Our last step consists into taking the scaling limit  $L_A, t \rightarrow \infty$ ; keeping the ratio  $t/L_A = \text{const} < 1/2$ , in such a way that the two edges of the subsystem  $A$  are not causally connected. In this limit, the  $L_A - 2t - 1$  MPS transfer matrices in between the two triangles in (32) can be substituted by the projector on their largest eigenvalue; explicitly we can write

$$\lim_{m \rightarrow \infty} \left( \frac{1}{d^n} \text{Diagram 3} \right)^m = \frac{1}{\chi^n} \text{Diagram 4}, \quad (33)$$

which allows to simplify Eq. (32) as

$$\text{tr} [\rho_A^n] = \left( \frac{1}{\chi^n d^{n(2t+1)}} \text{Diagram 5} \right)^2, \quad (34)$$

leading to Eq. (17).

### III. SPECTRUM OF $\tilde{U}\tilde{U}^\dagger$

In this section we want to study the spectrum of  $\tilde{U}\tilde{U}^\dagger$ , where  $\tilde{U}$  is obtained by a reshuffling of the indexes of the gate  $U$ , explicitly

$$\langle kl | \tilde{U} | ij \rangle = \langle lj | U | ki \rangle. \quad (35)$$

Since it is convenient to use diagrammatic calculus for our calculations here, we begin by introducing a few more useful diagrams. We represent a single gate as

$$\langle kl | U | ij \rangle \equiv \text{Diagram 6} = \left( \text{Diagram 7} \right)^*. \quad (36)$$

Therefore, unitarity and DU2 property (2) correspond to

$$\text{Diagram 8} = \text{Diagram 9} = \text{Diagram 10} = \text{Diagram 11} = \text{Diagram 12} = \text{Diagram 13}. \quad (37)$$

In fact, DU2 also implies

$$\text{Diagram 14} = \text{Diagram 15} = \text{Diagram 16} = \text{Diagram 17}. \quad (38)$$

The matrix  $\tilde{U}\tilde{U}^\dagger$  is clearly Hermitian, so it can be decomposed into orthogonal eigenspaces, with eigenvalues  $\Lambda^2$  which are the squared singular values of  $\tilde{U}$  with associated projector  $P_\Lambda$ . In formulae, this reads as

$$\tilde{U}\tilde{U}^\dagger = \text{[Diagram: A red square and a blue square connected by two lines, with four external lines]} \equiv \sum_{\Lambda} \Lambda^2 P_{\Lambda} \quad (39)$$

Now consider the following quantity, obtained taking the partial trace of  $(\tilde{U}\tilde{U}^\dagger)^n$

$$A = \text{[Diagram: A chain of n red and blue squares connected by lines, with four external lines]} = \sum_{\Lambda} \Lambda^{2n} \text{[Diagram: A box labeled } P_{\Lambda} \text{ with four external lines]} \quad (40)$$

Using Eq. (38) multiple times, we can rewrite Eq. (40) as

$$A = \frac{1}{d} \text{[Diagram: A chain of n red and blue squares connected by lines, with four external lines, and a dashed line connecting the top and bottom lines]} \quad (41)$$

Next, using (the complex conjugate of) Eq. (38) we find

$$\begin{aligned} A &= \frac{1}{d} \text{[Diagram: A chain of n red and blue squares connected by lines, with four external lines, and a dashed line connecting the top and bottom lines]} = \frac{1}{d} \text{[Diagram: A chain of n red and blue squares connected by lines, with four external lines, and a dashed line connecting the top and bottom lines, with a solid line connecting the top and bottom lines]} = \\ &= \frac{\mathbb{1}_d}{d} \sum_{\Lambda} \Lambda^{2n} \text{tr}[P_{\Lambda}], \end{aligned} \quad (42)$$

where unitarity was used in the last step. Comparing Eqs. (40) and (42), we get immediately

$$\text{[Diagram: A box labeled } P_{\Lambda} \text{ with four external lines]} = \frac{\text{tr}[P_{\Lambda}] \mathbb{1}_d}{d}, \quad \forall \Lambda. \quad (43)$$

With a completely analogous reasoning we can also obtain

$$\text{[Diagram: A box labeled } P_{\Lambda} \text{ with four external lines]} = \frac{\text{tr}[P_{\Lambda}] \mathbb{1}_d}{d}, \quad \forall \Lambda.. \quad (44)$$

Now consider

$$B = \text{[Diagram: A chain of n red and blue squares connected by lines, with four external lines]} = \sum_{\Lambda} \Lambda^{2n} \text{tr}[P_{\Lambda}] \quad (45)$$

Using Eqs. (37)  $m+1$  times, we get

$$B = \frac{1}{d} \text{[Diagram: A chain of n red and blue squares connected by lines, with four external lines, and a dashed line connecting the top and bottom lines]} \quad (46)$$

then, using Eq (38)  $m$  times ( $m=1$  in the diagram) we find

$$B = \frac{1}{d} \text{[Diagram: A chain of n red and blue squares connected by lines, with four external lines, and a dashed line connecting the top and bottom lines]} \quad (47)$$

where now we have  $n - m$  blue gates on the bottom and  $m + 1$  on top. Using Eqs. (40) and (43), we can simplify the gates on top to write

$$\begin{aligned}
 B &= \sum_{\Lambda} \Lambda^{2(m+1)} \frac{\text{tr}[P_{\Lambda}]}{d^2} \text{ (diagram with 6 gates: 3 blue on bottom, 3 red on top) } = \\
 &= \sum_{\Lambda, \Lambda'} \Lambda'^{2(n-m)} \Lambda^{2(m+1)} \frac{\text{tr}[P_{\Lambda}] \text{tr}[P_{\Lambda'}]}{d^2}.
 \end{aligned} \tag{48}$$

Combining Eqs. (45) and (48), we get

$$\forall n, m \quad \sum_{\Lambda, \Lambda'} \Lambda'^{2(n-m)} \Lambda^{2(m+1)} \frac{\text{tr}[P_{\Lambda}] \text{tr}[P_{\Lambda'}]}{d^2} = \sum_{\Lambda} \Lambda^{2n} \text{tr}[P_{\Lambda}] \tag{49}$$

which implies there can be only one nonzero  $\Lambda$ . In turn, this implies

$$\text{tr}[P_{\Lambda}] \Lambda = d^2 \quad \text{tr}[(\tilde{U}\tilde{U}^{\dagger})^n] = \Lambda^{2(n-1)} d^2 \tag{50}$$

Substituting (50) in (21) and setting  $n_{\Lambda} = \text{tr}[P_{\Lambda}]$  this gives Eq. (22).

#### IV. PARAMETERISATION FOR NUMERICAL EXPERIMENTS

In order to produce the plots in Fig. 3, we used a DU2 gate with  $d = 2$  and  $n_{\Lambda} = 2$ , parameterized as follows

$$U = u_0(v_1 \otimes v_2), \tag{51}$$

$$u_0 = \begin{pmatrix} e^{i\pi/4} & 0 & 0 & 0 \\ 0 & 0 & e^{-i\pi/4} & 0 \\ 0 & e^{-i\pi/4} & 0 & 0 \\ 0 & 0 & 0 & e^{i\pi/4} \end{pmatrix}, \quad v_{1/2} = \frac{1}{\sqrt{2}} \begin{pmatrix} e^{i\alpha_{1/2}} & -e^{-i\alpha_{1/2}} \\ e^{i\alpha_{1/2}} & e^{-i\alpha_{1/2}} \end{pmatrix}, \tag{52}$$

where the  $\alpha$ s have been fixed to the values  $\alpha_1 = 0.2, \alpha_2 = 0.3$ . The initial states chosen are random dimer states

$$|\Psi_0\rangle = \left( \sum_{i,j} m_{ij} |i, j\rangle \right)^{\otimes L}, \tag{53}$$

where the matrix  $m_{ij}$  is the normalized matrix whose elements, in the computation basis, are pseudo-random numbers distributed uniformly in  $[0, 1]$ .